

# Electronic structure of $\text{CaCu}_2\text{O}_3$ : Spin ladder versus one-dimensional spin chain

Esther Bordas, Coen de Graaf,\* and Rosa Caballol

*Departament de Química Física i Inòrganica, Universitat Rovira i Virgili, Plaça Imperial Tàrraco 1, 43005 Tarragona, Spain*

Carmen J. Calzado

*Departamento de Química Física, Universidad de Sevilla, c/Prof. García González s/n, 41012 Sevilla, Spain*

(Received 20 April 2004; revised manuscript received 14 September 2004; published 11 January 2005)

Quantum chemical calculations on embedded cluster models have been performed to extract accurate estimates of the magnetic coupling  $J$  and hopping parameters  $t$  of  $\text{CaCu}_2\text{O}_3$ . It is shown that this copper oxide compound is best described as a quasi-one-dimensional spin chain with weak interchain interactions within and between the  $\text{Cu}_2\text{O}_3$  planes. This magnetic structure is not reflected in the hopping parameters, since we find a large interplane hopping. Hence, the use of the simple second-order expression that relates  $J$ ,  $t$ , and the on-site repulsion  $U$  ( $J = -4t^2/U$ ) is not justified in all cases.

DOI: 10.1103/PhysRevB.71.045108

PACS number(s): 75.30.Et, 74.25.Jb, 75.10.Dg, 75.50.Ee

## I. INTRODUCTION

The spin ladders form a group of compounds with a wide variety of interesting phenomena. In relation to high-critical-temperature superconductivity, copper oxide spin ladders have received a lot of attention since the publication of the crystal structure of  $\text{SrCu}_2\text{O}_3$  and derivatives by Hiroi and co-workers<sup>1</sup> in 1991. The even-legged ladders in this series of compounds show spin-gap behavior and finite spin-spin correlation length, while the odd-legged ladders behave as isolated spin chains.<sup>2,3</sup> Beside these planar copper oxide spin ladders, other compounds with similar characteristics have been described in the literature ( $\text{La,Ca,Sr}_{14}\text{Cu}_{24}\text{O}_{41}$  and  $\text{LaCuO}_{2.5}$  being the most important ones.<sup>4-6</sup> The first one exhibits  $\text{Cu}_2\text{O}_3$  spin ladder planes similar to  $\text{SrCu}_2\text{O}_3$  combined with  $\text{CuO}_2$  spin chain layers, whereas in the latter compound the ladders are oriented in such a way that large interladder coupling can be expected which gives rise to a three-dimensional magnetic network with long-range order below  $\sim 110$  K.<sup>7</sup>

Recently, Kiryukhin and co-workers discussed the magnetic properties of the structurally related  $\text{CaCu}_2\text{O}_3$ .<sup>8</sup> The buckling of the spin ladder  $\text{Cu}_2\text{O}_3$  planes in this compounds reduces the magnetic interactions along the rungs of the ladder, and it was argued that  $\text{CaCu}_2\text{O}_3$  is actually not a spin ladder, but should be considered as a quasi-one-dimensional (quasi-1D) spin-1/2 chain. Consequently, a phase transition is observed at  $\sim 25$  K, where magnetic ordering sets in. The dominant magnetic interaction is along the legs of the ladders ( $J_{leg}$ ) in the  $b$  direction of the crystal (see Fig. 1). The high-temperature magnetic susceptibility was fitted with the theoretical expression for a 1D spin-1/2 chain based on the Bethe ansatz with a  $J$  value of  $-170$  meV. Weaker interactions of about 10 meV were assumed along the rung ( $J_{rung}$ ) and along the  $c$  direction between different ladder planes ( $J_c$ ). The interladder interaction within the spin ladder planes ( $a$ - $b$  planes) was argued to be of less importance, being highly frustrated. The Néel temperature ( $T_N$ ) is significantly higher than in  $\text{Sr}_2\text{CuO}_3$  (5.4 K) and  $\text{Ca}_2\text{CuO}_3$  (11 K), for which the interchain magnetic interactions are of the order of  $-1$  meV.<sup>9,10</sup>

Based on x-ray absorption spectroscopy combined with density functional theory (DFT) calculations, Kim *et al.* make an attempt to quantify more precisely the magnetic interactions in  $\text{CaCu}_2\text{O}_3$ .<sup>11</sup> The DFT calculations are performed within the local density approximation  $+U$  (LDA  $+U$ , where  $U$  is the on-site repulsion energy for two electrons on the same Cu atom). By fitting the resulting band structure, the hopping parameters were determined along the rung ( $t_{rung} \sim 250$  meV) and in the  $c$  direction between different spin ladder planes ( $t_c \sim 125$  meV). From the simple superexchange expression  $J = -4t^2/U$ , the authors estimate the corresponding magnetic coupling parameters. Using  $U \sim 3-5$  eV, they arrive at  $J_{rung} \sim -50$  meV and  $J_c \sim \pm 20$  meV. With a ratio  $J_{rung}/J_{leg} = 0.3$ , a pseudoladder magnetic structure is proposed and the authors ascribe the disappearance of the spin gap to the relatively large magnetic interaction between different ladder planes.

Quantum chemical calculations on embedded clusters are used here to further quantify the magnetic interaction and hopping parameters in  $\text{CaCu}_2\text{O}_3$ . The methodology solves as accurate as possible the exact (nonrelativistic) Hamiltonian

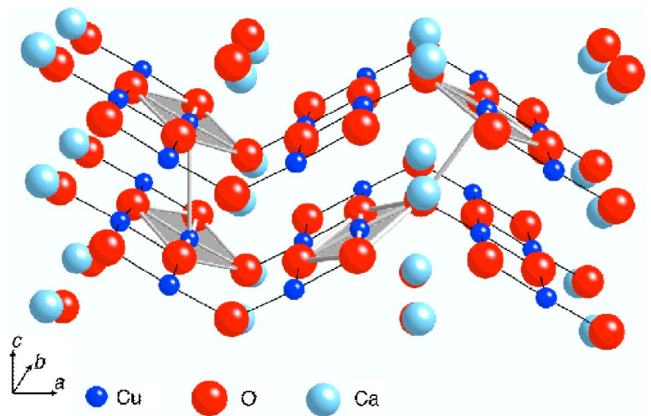


FIG. 1. (Color online) Crystal structure of  $\text{CaCu}_2\text{O}_3$ . Thick gray lines connect the cluster atoms used to compute the two different interplane interactions. The  $c, 1$  and  $c, 2$  interaction paths are schematically depicted on the left and right sides, respectively.

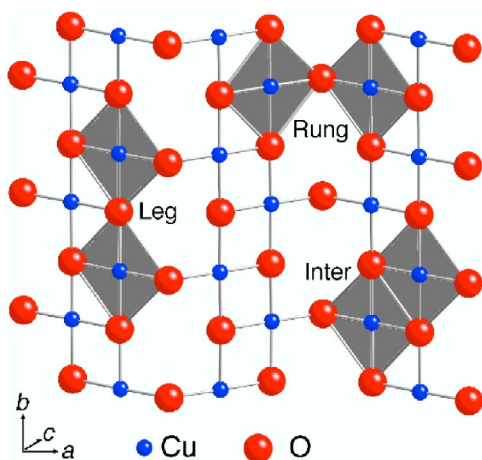


FIG. 2. (Color online) Schematic representation of the two-center clusters in the  $a$ - $b$  plane.

within the material model defined by the embedded cluster. In this way, the important electron correlation effects present in many transition metal compounds can be treated very accurately, and electronic structure parameters can be derived without any further assumption. This *ab initio* computational strategy has been applied very successfully over the last ten years and has reproduced, clarified, and even predicted the magnetic interaction and hopping parameters in many transition metal compounds (see Refs. 12–21 and references therein).

## II. COMPUTATIONAL INFORMATION

The clusters used in the calculation of the electronic structure parameters contain two or four copper atoms and all oxygens coordinating them. Figure 2 shows the two-center clusters that are used to determine the interactions along the rung and leg and between ladders in the  $a$ - $b$  plane. The clusters used to extract information about the interactions between magnetic centers in different  $a$ - $b$  planes are depicted in Fig. 1. The four-center cluster contains four Cu atoms placed on the same ladder in a rectangular geometry and all the oxygens coordinated to them. All clusters are embedded in optimized point charges (OPC's) that represent the Madelung potential due to the rest of the crystal. This Madelung potential is calculated by an Ewald summation assuming formal ionic point charges: i.e.,  $2+$  for Cu and Ca and  $2-$  for O. The optimized point charges reproduce the exact Madelung potential on a dense grid in the cluster region with a standard deviation less than 0.1 meV. The choice of formal ionic charges is consistent with the assignment of an integer number of electrons to the cluster to ensure overall charge neutrality. Furthermore, there exists by now substantial evidence in the literature that the electronic structure parameters considered here do not critically depend on the value of the charges to calculate the Madelung potential.<sup>22–24</sup> This observation only holds for ionic transition metal compounds. In case of materials with covalent bonds such as  $\text{CuGeO}_3$ , the embedding procedure with formal charges does not lead to meaningful results and alternative embedding schemes

should be applied.<sup>25,26</sup> In the results section, we will shortly come back to the influence of the Madelung potential on the properties studied here.

To avoid artificial polarization of the electronic charge distribution due to the cluster atoms towards the point charges, total ion potentials<sup>27</sup> (TIP's) replace the point charges on the boundary of the cluster. These TIP's account for the Coulomb and exchange interactions between the cluster atoms and the atoms directly around it. The  $\text{Ca}^{2+}$  TIP corresponds to the large core potential of Durand and Barthelat<sup>28</sup> and the  $\text{Cu}^{2+}$  TIP is a modification of the original large core potential to include the  $3d$  shell in the potential.<sup>29</sup> The geometry of the cluster has been taken from experiment.<sup>8</sup>

The validity of the embedded cluster model to extract electronic structure parameters in ionic transition metal compounds has been established in two ways. In the first place, several studies have been published that contrast embedded cluster results with periodic calculations. In all cases, the calculated values are very similar given that the approximation to the  $N$ -electron wave function is identical in both approaches.<sup>30–33</sup> Second, cluster size effects have been studied before in other cuprates ( $\text{Li}_2\text{CuO}_2$ ,  $\text{Sr}_2\text{CuO}_3$ , and  $\text{La}_2\text{CuO}_4$ ) and nickel compounds ( $\text{NiO}$ ,  $\text{KNiF}_3$ , and  $\text{K}_2\text{NiF}_4$ ) by comparing results obtained with two, three, four, and even five magnetic centers. In none of these cases significant effects were observed.<sup>10,18,19,34</sup>

Two different computational schemes have been applied to approximate the exact  $N$ -electron wave function of the cluster electrons. The first scheme is the complete active-space self-consistent field (CASSCF), which simultaneously optimizes the spatial extent of the orbitals and the wave function expansion in the space spanned by the  $N$ -electron configurations that can be constructed by distributing the unpaired electrons in all possible ways over the active orbitals. For the undoped clusters, the active orbitals are mainly localized on the copper centers although they show some delocalization onto the neighboring oxygen ions. The two-center cluster CAS contains two orbitals and two electrons. In the four-center cluster, there are four magnetic orbitals and four electrons in the CAS. For the doped clusters, we used active spaces with one electron less. The active orbitals turn out to be more delocalized with large contributions from the neighboring O  $2p$  orbitals.<sup>35</sup>

The CASSCF approach accounts for the direct exchange  $K$  between the two magnetic centers and the kinetic exchange  $-4t^2/U$ . However, this description of the electronic structure leads to a severe overestimation of  $U$  and, consequently, too small magnetic coupling parameters. Second, we include the remaining electron correlation effects such as spin polarization, ligand to metal charge transfer configurations, etc. (see Ref. 36 for a detailed discussion) with the difference dedicated configuration interaction (DDCI). This method is specially designed to obtain accurate relative energies of different electronic states<sup>37</sup> and has been proven to give magnetic interaction parameters in close agreement with experiment. The molecular orbital set is obtained by means of the iterative DDCI (IDDCI) scheme<sup>38</sup> to avoid any possible bias toward one of the electronic states. In this approach, an average density matrix is constructed from the

TABLE I. CASSCF and IDDCI magnetic coupling  $J$  and hopping parameters  $t$  (in meV) for  $\text{CaCu}_2\text{O}_3$ .

	$d(\text{Cu-Cu})$	Magnetic coupling		Hopping	
		CASSCF	IDDCI	CASSCF	IDDCI
Inter	2.8 Å	3.0	24.3	-124	-143
Rung	3.3 Å	-1.9	-11.3	-250	-244
$c,1$	3.5 Å	0.02	0.09	-16	-2.8
Leg	4.1 Å	-24.0	-134.1	-720	-622
$c,2$	4.8 Å	0.09	0.75	-122	-134
Diag	5.3 Å	-0.04	-0.16	-14	-30

DDCI density matrices of all electronic states. The vectors that are obtained from the diagonalization of this average density matrix serve as input for a new DDCI cycle. The procedure is repeated until convergence, what usually happens within four to six iterations.

The basis set to expand the one-electron functions have the following characteristics: The Cu ( $2s, 14p, 10d, 4f$ ) primitive set is contracted to ( $6s, 5p, 4d, 1f$ ) functions, and the O ( $14s, 9p, 4d$ ) primitive set is contracted to ( $4s, 3p, 1d$ ) functions.<sup>39,40</sup> Calculations have been performed with MOLCAS5.4 (Ref. 41) and CASDI (Ref. 42).

### III. RESULTS

#### A. Magnetic coupling

Table I lists the magnetic coupling and hopping parameters ordered by increasing Cu-Cu interatomic distance. Beside the usual in-plane interactions along the leg and rung and between copper atoms situated on different ladders ( $J_{inter}$  and  $t_{inter}$ ), we also investigated two different interplane interactions. The interaction between copper atoms in different planes separated by 3.5 Å along the  $c$  axis (see Fig. 1, on the left) is labeled with the subscript  $c,1$ . A second possible interaction pathway is shown on the right in Fig. 1 and is referred to with the subscript  $c,2$ . Although the copper atoms are further separated in space, the relative orientation of the  $\text{CuO}_4$  units with an oxygen atom connecting both metallic centers could be more favorable for magnetic interaction and hopping processes than along the  $c,1$  path parallel to the  $c$  axis. To complete the discussion, we also mention the in-plane interactions along the diagonal of the  $\text{Cu}_4\text{O}_{12}$  plaquettes.<sup>43</sup>

The corner sharing  $\text{CuO}_4$  squares along the legs of the ladders provide the optimum geometry for a strong magnetic coupling. Both for CASSCF and IDDCI, the coupling along the leg gives indeed the largest magnetic interaction. For CASSCF, we find -24 meV, but the inclusion of electron correlation effects strongly enhances the magnitude of the coupling. Our final IDDCI estimate of the coupling is -134 meV (1610 K). The experimental estimate based on the fitting of the temperature dependence of the magnetic susceptibility [ $\chi(T)$ ] is  $-160 \pm 25$  meV ( $1950 \pm 300$  K).<sup>8</sup> Our *ab initio* estimate is on the lower limit of this range, but in the fitting of the experimental data only the interaction along

the leg was considered; the influence of other magnetic interactions on  $\chi(T)$  was not accounted for.

The interaction along the rung is much weaker because of the distorted Cu-O<sub>r</sub>-Cu bond (O<sub>r</sub> is the oxygen located on the rung) with an angle of 123°. The buckling of the ladder planes makes the ratio  $J_{rung}/J_{leg}$  calculated with IDDCI less than 0.1, whereas it is close to 1 in the structurally related spin ladder compound  $\text{SrCu}_2\text{O}_3$ . In a computational experiment, we gradually restore the linearity of the Cu-Cu linkage along the rung by varying the Cu-O<sub>r</sub>-Cu angle at fixed distances. The embedding is kept frozen. As expected,  $J_{rung}$  increases monotonically with increasing bond angle and  $J_{rung}/J_{leg}$  approaches 0.3, as proposed in Ref. 11, for 140°. For angles as large as 170°, the ratio is 0.7, still significantly smaller than 1.

To study the stability of the results with respect to the Madelung potential, we varied the value of the embedding point charges around the formal ionic value of  $\pm 2$  by increasing and decreasing them with 20%. In line with previous findings,<sup>22-24</sup>  $J_{rung}$  is found to be rather stable with the variation of the Madelung potential. It varies between -13.2 meV and -9.5 meV for the reduced and increased point charges, respectively.

The interladder interaction in the  $\text{Cu}_2\text{O}_3$  planes is ferromagnetic and about twice as large as the rung coupling. However, it has recently been mentioned that IDDCI possibly slightly overestimates ferromagnetic couplings,<sup>24,44</sup> and the present value of 24 meV should be taken as an upper limit. The remaining magnetic coupling within the ladder planes  $J_{diag}$  has been calculated from a four-center cluster. Calzado and Malrieu showed that the energy eigenvalues of the spin wave function no longer give sufficient information and  $J_{diag}$  can only be determined with the help of effective Hamiltonians.<sup>18</sup> The resulting value for  $J_{diag}$  is much smaller than those found in  $\text{La}_2\text{CuO}_4$  (Ref. 18) and  $\text{SrCu}_2\text{O}_3$  (Ref. 43), which again can be ascribed to the buckling of the ladder planes.

The lack of a bridging ligand and the relative orientation of the  $\text{CuO}_4$  units make the magnetic coupling along the  $c$  axis very weak. The  $\text{CuO}_4$  plaquettes involved in  $J_{c,1}$  are stacked in a parallel way, comparable to the interchain coupling in the above-mentioned 1D spin chains  $\text{Sr}_2\text{CuO}_3$  and  $\text{Ca}_2\text{CuO}_3$ . In the present case, however, the  $\text{CuO}_4$  units are displaced with respect to each other by approximately 1.8 Å. This makes the overlap between the magnetic orbitals (mainly of Cu  $3d_{x^2-y^2}$  character) even less favorable and  $J_{c,1}$

TABLE II. On-site repulsion energy (in eV) for different copper oxide compounds estimated from  $-4t^2/J$  using IDDCI parameters ( $U_{pert}$ ) and calculated with IDDCI ( $U_{var}$ ).

Compound	$t$ (meV)	$J$ (meV)	$U_{pert}$	$U_{var}$
CaCu <sub>2</sub> O <sub>3</sub>				
Inter	-143	24.3	3	5.8
Rung	-244	-11.3	21	6.7
$c,1$	-3	0.09	3	
Leg	-622	-134.1	12	6.5
$c,2$	-134	0.75	96	
La <sub>2</sub> CuO <sub>4</sub> <sup>a</sup>	-598	150	9.5	7.3
Li <sub>2</sub> CuO <sub>2</sub> <sup>b</sup>				
NN	-143	12.2	6.7	
NNN	120	1.9	26	
Sr <sub>2</sub> CuO <sub>3</sub> <sup>c</sup>				
In-chain	659	-246	7.1	
Inter	30	-0.44	8.3	

<sup>a</sup>Values taken from Refs. 33, 35, and 48.

<sup>b</sup>Values refer to in-chain nearest-neighbor (NN) and next-nearest-neighbor (NNN) interactions (Ref. 19).

<sup>c</sup>Values taken from Ref. 10.

(IDDCI) is less than 0.1 meV ( $\sim 1$  K), which is significantly smaller than the  $\sim -1$  meV for Sr<sub>2</sub>CuO<sub>3</sub> and Ca<sub>2</sub>CuO<sub>3</sub>. The relative orientation of the CuO<sub>4</sub> units is rather different for  $J_{c,2}$ . Despite the larger Cu-Cu interatomic distance,  $J_{c,2}$  is larger than  $J_{c,1}$ . This is in line with the observation that the magnetic orbitals are no longer parallel and the rung oxygen provides some type of bridge between the two copper atoms involved in the magnetic coupling parametrized by  $J_{c,2}$ .

### B. Hopping parameters

The differences in CASSCF and IDDCI hopping parameters listed in Table I are less pronounced than for the magnetic coupling parameters. The insensitivity of the hopping parameter to the exact details of the electron correlation treatment has been observed before for other systems<sup>10,45</sup> and implies that this parameter is essentially a one-electron property. This allows us to compare our cluster model IDDCI estimates to those obtained from the periodic calculations by Kim *et al.* within the LDA+ $U$  scheme.<sup>11</sup>

The largest hopping is found along the legs of the ladders. The IDDCI value ( $-622$  meV) is comparable to the hopping along similar Cu-O-Cu bonds found in the two-dimensional antiferromagnets La<sub>2</sub>CuO<sub>4</sub> (Ref. 35) and related cuprates (Ref. 33). Whereas  $J_{rung}$  is more than 10 times smaller than  $J_{legs}$ , the corresponding hopping parameter is only smaller by a factor of 2.5. The IDDCI estimate of  $-244$  meV is in remarkable good agreement with the LDA+ $U$  value of  $\sim 250$  meV proposed for the rung.

The interplane hopping parameters can only be obtained from the mapping of the IDDCI wave functions onto an effective Hamiltonian. The lack of an inversion center in the Cu<sub>2</sub>O<sub>8</sub> clusters (two CuO<sub>4</sub> plaquettes in different ladder planes) makes that the energy eigenvalues of the two lowest doublet states are not sufficient to calculate  $t$ . The difference

observed for the magnetic interactions along the pathways  $c,1$  and  $c,2$  is more pronounced for the hopping parameters:  $t_{c,1}$  is very small, only  $-3$  meV, while  $t_{c,2}$  is an order of magnitude larger and similar to the in-plane interladder hopping  $t_{inter}$ . These results suggest that the band dispersion in the  $c$  direction observed by Kim *et al.* is due to the hopping of electrons (or holes) between CuO<sub>4</sub> plaquettes with a relative orientation as shown on the right in Fig. 1—i.e., the  $c,2$  interaction path. Our interplane hopping ( $t_{c,2} = -134$  meV) is again very close to the LDA+ $U$  value of  $\sim 125$  meV. Finally, we find a hopping parameter of  $-30$  meV along the diagonal of the buckled Cu<sub>4</sub>O<sub>12</sub> plaquettes. This interaction should probably also be included in a simulation of the macroscopic properties of CaCu<sub>2</sub>O<sub>3</sub>.

### C. Validity of the superexchange relation

With the *ab initio* values for  $t$  and  $J$  at hand, the question arises to what extent the simple superexchange relation  $U = -4t^2/J$  can be used to estimate one of the three parameters once the other two are known. Several examples can be found in the literature where assumptions about the relative size of different  $J$ 's have been made solely based on the magnitude of the hopping parameters. Beside for CaCu<sub>2</sub>O<sub>3</sub>, this strategy has also been applied for Li<sub>2</sub>CuO<sub>2</sub> and Li<sub>2</sub>VOSiO<sub>4</sub>.<sup>46,47</sup> Table II recompiles the estimates of  $U$  based on the superexchange formula ( $U_{pert}$ ) using  $J$  and  $t$  obtained with IDDCI. We add the values for La<sub>2</sub>CuO<sub>4</sub>, Li<sub>2</sub>CuO<sub>2</sub>, and Sr<sub>2</sub>CuO<sub>3</sub>. The on-site repulsion parameter can also be determined variationally from quantum chemical calculations by means of the projection of the IDDCI wave functions onto an effective Hamiltonian as outlined in Ref. 48. We use  $U_{var}$  for the values obtained by this more accurate procedure.

It is readily seen that the applicability of the formula is not universal. For nearest-neighbor interactions along (al-

most) lineal Cu-O-Cu bonds,  $U_{pert}$  is at most of the right order of magnitude. For other type of interactions, the  $U_{pert}$  estimates show a large dispersion and unphysical values as large as 96 eV are obtained for the interaction in  $\text{CaCu}_2\text{O}_3$  along  $c$ .<sup>2</sup>  $U_{var}$  is related (but not equal) to the energy difference between the neutral state (with mainly Cu  $3d^9$ -O  $2p^6$ -Cu  $3d^9$  contributions) and the ionic state (mainly Cu  $3d^{10}$ -O  $2p^6$ -Cu  $3d^8$ ). The variational determined on-site repulsion parameters for  $\text{CaCu}_2\text{O}_3$  obtained with different clusters are more consistent than those calculated with the superexchange relation. We obtain  $U_{var}=5.8, 6.7,$  and  $6.5$  eV for the in-plane interladder, the rung, and the leg clusters, respectively.

The failure of the perturbative expression to relate  $t$  with  $J$  shows that the reduction of the magnetic coupling constant to its kinetic exchange compound is too crude an approximation. In the first place, it should be noted that within the Anderson model, the magnetic coupling  $J$  is the sum of a ferromagnetic term  $J^F$ , generally ascribed to direct exchange, and an antiferromagnetic term  $J^{AF}$  due to the kinetic exchange. Hence, strictly speaking, the superexchange formula only relates  $t$  with the antiferromagnetic component and not to the magnetic coupling itself. Second, the hopping parameter  $t$  as determined from doped clusters does not have exactly the same meaning as the  $t$  in the superexchange relation. In the latter relation,  $t$  is related to the Hamilton matrix element between the neutral and the ionic states,<sup>48</sup> while it parametrizes the mobility of the holes in the cluster calculations. The same holds for the values derived from the LDA band structure calculations.

#### IV. CONCLUSIONS

The IDDCI magnetic interactions parameters suggest that  $\text{CaCu}_2\text{O}_3$  is best described as a quasi-1D spin chain. The chains are coupled in the  $a$  direction through the distorted rungs and nonzero interplane interactions along the  $c$  axis, especially  $J_{c,2}$ . These interactions can be at the origin of the

long-range ordering below the Néel temperature. The magnetic structure of the compound is, however, not as simple as the related  $\text{Ca}_2\text{CuO}_3$ . In that case the mean-field expression<sup>49</sup> that relates the magnetic in-chain and interchain coupling parameters to  $T_N$  gives very reasonable results for the DDCI parameters.<sup>10</sup> The application of the same equation for  $\text{CaCu}_2\text{O}_3$  leads to an overestimation of  $T_N$  by at least an order of magnitude. Obviously, other interactions than  $J_{rung}$  and  $J_{c,2}$  also play a role in the magnetic structure. The role of the frustrated in-plane interladder interaction is expected to be small. The quantum Monte Carlo simulations of Johnston *et al.* for the planar spin ladder  $\text{SrCu}_2\text{O}_3$  suggest that this coupling does not influence the magnetic susceptibility up to  $J_{inter}/J_{leg}=0.2$ .<sup>50</sup> The four-body cyclic exchange (estimated with *ab initio* calculations<sup>43</sup> to be 4 meV) and  $J_{diag}$  may play an important role in the magnetic structure.

The close resemblance between the theoretical estimates of  $t$  from a periodic modelization of the crystal (the LDA +  $U$  calculations of Kim *et al.*<sup>11</sup>) and from a cluster model approach (the present IDDCI estimates) gives additional evidence of the appropriateness of the local model to extract this type of parameters.

An interesting observation from the calculations is that the magnetic structure cannot be directly extracted from the size of the hopping parameters along the different interaction paths. The magnetic interaction along the  $c$  axis is much smaller than can be expected at first sight from the size of the hopping parameter. This behavior is not unique for  $\text{CaCu}_2\text{O}_3$  but has also been observed for other cuprates—e.g.,  $\text{Li}_2\text{CuO}_2$ . We conclude that only for similar interaction paths, the magnitude of  $t$  serves as a guide for the relative size of the corresponding magnetic couplings.

#### ACKNOWLEDGMENTS

Financial support has been provided by the Spanish Ministry of Science and Technology under Project No. BQU2002-04029-C02-02 and the DURSI of the Generalitat de Catalunya (Grant No. SGR01-00315)

\*Electronic address: coen@correu.urv.es

<sup>1</sup>Z. Hiroi, M. Azuma, M. Takano, and Y. Bando, *J. Solid State Chem.* **95**, 230 (1991).  
<sup>2</sup>T. M. Rice, *Z. Phys. B: Condens. Matter* **103**, 165 (1997).  
<sup>3</sup>E. Dagotto, *Rep. Prog. Phys.* **62**, 1525 (1999).  
<sup>4</sup>T. Siegrist, S. M. Zahurak, D. W. Murphy, and R. S. Roth, *Nature (London)* **334**, 231 (1988).  
<sup>5</sup>E. M. McCarron III, M. A. Subramanian, J. C. Calabrese, and R. L. Harlow, *Mater. Res. Bull.* **23**, 1355 (1988).  
<sup>6</sup>Z. Hiroi and M. Takano, *Nature (London)* **377**, 41 (1995).  
<sup>7</sup>S. Matsumoto, Y. Kitaoka, K. Ishida, K. Asayama, Z. Hiroi, N. Kobayashi, and M. Takano, *Phys. Rev. B* **53**, R11 942 (1996).  
<sup>8</sup>V. Kiryukhin, Y. J. Kim, K. J. Thomas, F. C. Chou, R. W. Erwin, Q. Huang, M. A. Kastner, and R. J. Birgeneau, *Phys. Rev. B* **63**, 144418 (2001).  
<sup>9</sup>H. Rosner, H. Eschrig, R. Hayn, S.-L. Drechsler, and J. Málek, *Phys. Rev. B* **56**, 3402 (1997).

<sup>10</sup>C. de Graaf and F. Illas, *Phys. Rev. B* **63**, 014404 (2001).

<sup>11</sup>T. K. Kim, H. Rosner, S.-L. Drechsler, Z. Hu, C. Sekar, G. Krabbes, J. Málek, M. Knupfer, J. Fink, and H. Eschrig, *Phys. Rev. B* **67**, 024516 (2003).  
<sup>12</sup>F. Illas, J. Casanovas, M. A. Garcia-Bach, R. Caballol, and O. Castell, *Phys. Rev. Lett.* **71**, 3549 (1993).  
<sup>13</sup>A. B. van Oosten, R. Broer, and W. C. Nieuwpoort, *Chem. Phys. Lett.* **257**, 207 (1996).  
<sup>14</sup>C. J. Calzado, J. F. Sanz, J.-P. Malrieu, and F. Illas, *Chem. Phys. Lett.* **307**, 102 (1999).  
<sup>15</sup>I. de P. R. Moreira, F. Illas, C. J. Calzado, J. F. Sanz, J.-P. Malrieu, N. Ben Amor, and D. Maynau, *Phys. Rev. B* **59**, R6593 (1999).  
<sup>16</sup>C. de Graaf, I. de P. R. Moreira, F. Illas, and R. L. Martin, *Phys. Rev. B* **60**, 3457 (1999).  
<sup>17</sup>D. Muñoz, F. Illas, and I. de P. R. Moreira, *Phys. Rev. Lett.* **84**, 1579 (2000).

- <sup>18</sup>C. J. Calzado and J.-P. Malrieu, *Phys. Rev. B* **63**, 214520 (2001).
- <sup>19</sup>C. de Graaf, I. de P. R. Moreira, F. Illas, O. Iglesias, and A. Labarta, *Phys. Rev. B* **66**, 014448 (2002).
- <sup>20</sup>N. Suaud and M.-B. Lepetit, *Phys. Rev. Lett.* **88**, 056405 (2002).
- <sup>21</sup>L. Hozoi, A. H. de Vries, A. B. van Oosten, R. Broer, J. Cabrero, and C. de Graaf, *Phys. Rev. Lett.* **89**, 076407 (2002).
- <sup>22</sup>C. Sousa, J. Casanovas, J. Rubio, and F. Illas, *J. Comput. Chem.* **14**, 680 (1993).
- <sup>23</sup>C. de Graaf, R. Broer, and W. C. Nieuwpoort, *Chem. Phys. Lett.* **271**, 372 (1997).
- <sup>24</sup>C. de Graaf, L. Hozoi, and R. Broer, *J. Chem. Phys.* **120**, 961 (2004).
- <sup>25</sup>T. Klüner, N. Govind, Y. A. Wang, and E. A. Carter, *J. Chem. Phys.* **116**, 42 (2002).
- <sup>26</sup>E. Ruiz, J. Cano, S. Alvarez, P. Alemany, and M. Verdguer, *Phys. Rev. B* **61**, 54 (2000).
- <sup>27</sup>N. W. Winter, R. M. Pitzer, and D. K. Temple, *J. Chem. Phys.* **86**, 3549 (1987).
- <sup>28</sup>P. Durand and J. C. Barthelat, *Theor. Chim. Acta* **38**, 283 (1975).
- <sup>29</sup>F. Illas, J. Rubio, and J. C. Barthelat, *Chem. Phys. Lett.* **119**, 397 (1985).
- <sup>30</sup>J. M. Ricart, R. Dovesi, C. Roetti, and V. R. Saunders, *Phys. Rev. B* **52**, 2381 (1995).
- <sup>31</sup>I. de P. R. Moreira and F. Illas, *Phys. Rev. B* **55**, 4129 (1997).
- <sup>32</sup>Y.-S. Su, T. A. Kaplan, S. D. Mahanti, and J. F. Harrison, *Phys. Rev. B* **59**, 10 521 (1999).
- <sup>33</sup>D. Muñoz, I. de P. R. Moreira, and F. Illas, *Phys. Rev. B* **65**, 224521 (2002).
- <sup>34</sup>F. Illas, I. de P. R. Moreira, C. de Graaf, O. Castell, and J. Casanovas, *Phys. Rev. B* **56**, 5069 (1997).
- <sup>35</sup>C. J. Calzado, J. F. Sanz, and J.-P. Malrieu, *J. Chem. Phys.* **112**, 5158 (2000).
- <sup>36</sup>C. J. Calzado, J. Cabrero, J.-P. Malrieu, and R. Caballol, *J. Chem. Phys.* **116**, 2728 (2002).
- <sup>37</sup>J. Miralles, J. P. Daudey, and R. Caballol, *Chem. Phys. Lett.* **198**, 555 (1992).
- <sup>38</sup>V. M. García, O. Castell, R. Caballol, and J.-P. Malrieu, *Chem. Phys. Lett.* **238**, 222 (1995).
- <sup>39</sup>P.-O. Widmark, P.-Å. Malmqvist, and B. O. Roos, *Theor. Chim. Acta* **77**, 291 (1990).
- <sup>40</sup>R. Pou-Américo, M. Merchán, I. Nebot-Gil, P.-O. Widmark, and B. O. Roos, *Theor. Chim. Acta* **92**, 149 (1995).
- <sup>41</sup>K. Andersson *et al.*, computer code MOLCAS, version 5.4, Department of Theoretical Chemistry, University of Lund, 2002.
- <sup>42</sup>D. Maynau and N. Ben Amor, CASDI suite of programs, Université Paul Sabatier, Toulouse, 1997.
- <sup>43</sup>C. J. Calzado, C. de Graaf, E. Bordas, R. Caballol, and J.-P. Malrieu, *Phys. Rev. B* **67**, 132409 (2003).
- <sup>44</sup>J. Cabrero, C. de Graaf, E. Bordas, R. Caballol, and J.-P. Malrieu, *Chem.-Eur. J.* **9**, 2307 (2003).
- <sup>45</sup>C. J. Calzado and J.-P. Malrieu, *Chem. Phys. Lett.* **317**, 404 (2000).
- <sup>46</sup>R. Weht and W. E. Pickett, *Phys. Rev. Lett.* **81**, 2502 (1998).
- <sup>47</sup>H. Rosner, R. R. P. Singh, W. H. Zheng, J. Oitmaa, and S.-L. Drechsler, *Phys. Rev. Lett.* **88**, 186405 (2002).
- <sup>48</sup>C. J. Calzado, J. Cabrero, J.-P. Malrieu, and R. Caballol, *J. Chem. Phys.* **116**, 3985 (2002).
- <sup>49</sup>H. J. Schulz, *Phys. Rev. Lett.* **77**, 2790 (1996).
- <sup>50</sup>D. C. Johnston *et al.*, cond-mat/0001147 (unpublished).